

V-shaped wing design and hydrodynamic analysis based on moving base for recovery AUV

Guiqiang Bai, Haitao Gu, Haiting Zhang, Lingshuai Meng, Dongsheng Tang

Abstract—Aiming at AUV capture and recovery, a moving base--V-shaped wing that can increase the recovery success rate of AUVs is designed in this paper. The Bernoulli equation of the ideal fluid is used as the design principle. The SolidWorks is used to design the V-shaped wing in three dimensions. The CFD simulation software is used to simulate the hydrodynamics of the V-shaped wing. Calculation results show that the V-shaped wing can generate down force and the resistance increases with the increase of speed. The V-shaped wing is 3D printed and the water test is conducted. When the towing speed is 2 knots, the V-shaped wing can generate 11N down force and can keep stability of the depth.

I. INTRODUCTION

Recovery AUVs using a moving base can reduce the risk for operation staff and even can achieve unmanned recovery. What's more, it can clear technical obstacles for the development of future marine unmanned systems.^[1] Zhejiang University, Woods Hole Oceanographic Institution and the University of Girona have been developed the fix base for the recovery of AUVs.^[2-4] Kongsberg also developed a stationary device for unmanned recovery RAMUS 100 AUV^[5]. Woods Hole Institute design a compact bottom-mounted docking station to recovery and recharge the RAMUS 100 AUV^[6]. Florida Atlantic University have conducted research on the recovery of AUVs using moving base technology, they design a moving base with two rope and an anchoring checker board

This work was supported by The Innovation Fund from Chinese Academy of Sciences (Grant No. CXJJ-17-M130); The Advance Research Fund of Science and Technology (Grant No. 3020605040302); The Joint Fund for Advance Research from Chinese Academy of Sciences (Grant No. 6141A01061601).

GQ Bai is with State Key Laboratory of Robotics, Shenyang Institute of Automation, Chinese Academy of Sciences, CO 110016 China, and University of Chinese academy of sciences, Beijing 100049. (e-mail: baiguiqiang@sia.cn).

HT Gu is with State Key Laboratory of Robotics, Shenyang Institute of Automation, Chinese Academy of Sciences, CO 110016 China. (phone:024-23970747 Fax : e-mail:ght@sia.cn).

HT Zhang is with Northeastern University, shenyang, CO 110819 China (e-mail: zhanghaiting@sia.cn).

LS Meng is with State Key Laboratory of Robotics, Shenyang Institute of Automation, Chinese Academy of Sciences, CO 110016 China, and University of Chinese academy of sciences, Beijing 100049. (e-mail: menglingshuai@sia.cn).

DS Tang is with State Key Laboratory of Robotics, Shenyang Institute of Automation, Chinese Academy of Sciences, CO 110016 China, and University of Chinese academy of sciences, Beijing 100049. (e-mail: tangdongsheng@sia.cn).

R. B. G. thanks Beijing municipal people's government, ministry of industry and information technology, China association of science and technology.

target, but this device will increase the resistance of AUVs^[7], and then they developed another moving base which could achieve the AUVs autonomous recovery^[8-10]. Lockheed Martin company design a moving base to recovery the Marlin AUV, the moving base was drag by the maned vehicle. What's more, when recovery the Marlin AUV, the moving base is almost statically, so it can not be towed by the USV^[11]. The Stennis Space Center of the Naval Oceanographic Office design a towing devices to recovery, but the device is too huge to install on USVs^[12]. Partial recovery towing device is shown in figure 1.

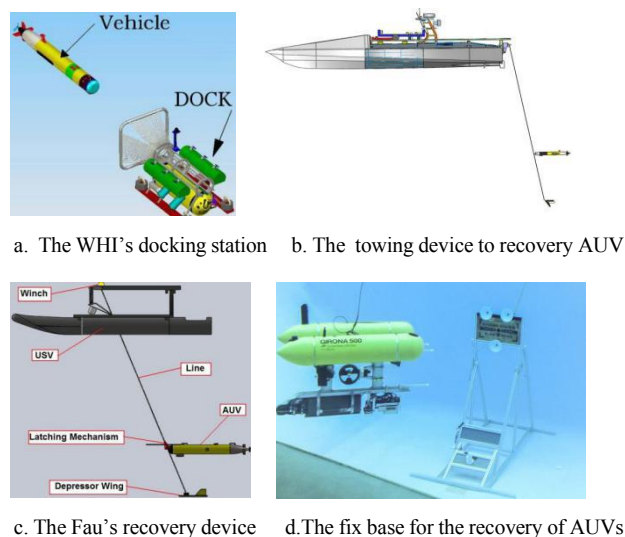


Fig 1. The towing device for the recovery of AUV

At present, most underwater towing devices are mainly controlled by rudders and equipped with sonars and other. They are usually used for detection applications. Their design makes them not suitable for working as a moving base for recovery AUVs. In 2014, the United States used Rolls-Royce's new underwater towing vehicle to search for the Malaysia Airlines MH370^[13]. AS the moving base needs to have a certain down force in addition to good stability, we designed the V-shaped wing inspired by the Rolls-Royce's vehicle.

II. THE DESIGN OF V-SHAPED WING

A. Background of V-shaped wing Design

The V-shaped wing is towed by the portable USV, as shown in figure 2, and the main parameters for portable USV as shown in table 1. The USV use the DGPS to locate the position and with the electronic compass for navigation. the portable USV could generate 100N tension.



Fig2. The portable USV

TABLE 1. The Main Parameters For Portable USV

Parameters	Magnitude
Mass	40kg
Length	1200mm
Maximum velocity	1.5m/s
Maximum pull	10kg

The primary objective of designing the V-shaped wing is to recover the handy AUV, as shown in figure 3, and the main parameters for handy AUV as shown in table 2. When the AUV need to be recovered, the docking mechanism which are installed on the AUV would capture the towing cable. So the cable should be stable and tense.



Fig3. The portable AUV

TABLE 2. The Main Parameters For Portable USV

Parameters	Magnitude
Mass	85kg
Length	2300mm
Maximum velocity	2m/s
Maximum submerged depth	50m

B. Background of V-shaped wing Design

When recover an AUV with a moving base, the base needs to generate down force to make the recovery cable tight and keep navigating stably. In view of the above two points, this paper designs a V-shaped wing, suitable for dynamic capture and recovery of AUVs. In this study, the AUV can navigate steadily at 1.5m/s. During the recovery process, the speed of the AUV must be faster than the moving base. To decrease the flow resistance, the dragging speed of the V-shaped wing is set to 1m/s. The environment of the fluid around the V-shaped wing can be considered as ideal fluid. The Bernoulli equation for ideal fluid is:

$$p_1 / \rho g + z_1 + \mu_1^2 / 2g = p_2 / \rho g + z_2 + \mu_2^2 / 2g \quad (1)$$

Where: p is the pressure generated by the fluid when it flows over the surface of the V-shaped wing, z is the height of the V-shaped wing surface in the water, while μ is stands for the speed of the fluid, ρ is the density of water.

The V-shaped wing needs to be designed following the rules below: the surface area of the lower surface is greater than that of the upper surface, so the flow rate of the water flowing on the upper surface is less than the lower ($\mu_1 < \mu_2$), so generating a downward pressure on the upper surface of the V-shaped wing ($p_1 > p_2$). Take the longitudinal dimension L of the V-shaped wing as the basic input, the width is D ; the total height is H ; the bottom raised height is d , the height of the tail wing is h , and the length is l . The relationship between the dimensions of each part of V wing is as equation (2):

$$D = 1.1L, H = 1/3L, d = 1/15L, h = 1/3H, l = 1/5L \quad (2)$$

Using S stands for the length of the USV, We set $S=1.2m$, and $L = 0.4S$, $L = 450mm$. Then the size of each part of the V-shaped wing will be: $D = 520mm$, $H = 150mm$, $d = 30mm$, $h = 50mm$, $l = 180mm$. The V-shaped wing is shown in figure 4.

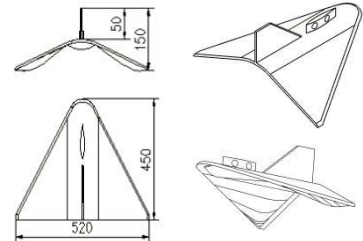


Fig 4. Three dimensional image

III.FORCE ANALYSIS

The torpedo-shaped AUV has good maneuverability in the smooth sea and poor maneuverability in the moderate sea^[14]. Therefore we choose smooth sea to recover the AUV. According to Table 3, the Beaufort Wind Scale, the wave height of slight sea state is 0.6-1m. The average wavelength in the slight sea state is 6.1 m, and the depth of the wave base plane in deep water is $0.5L_w$ ^[15]. In order to avoid the influence of waves and surface currents, the depth of AUV recovery should be greater than 3 meters.

TABLE 3. BEAUFORT WIND FORCE SCALE

Scale	Force rating	Wave	Wave height(m)
0	Clam	—	—
1	Light air	—	—
2	Light breeze	—	0.2—0.3
3	Gentle breeze	Slight	0.6—1
4	Moderate breeze	Slight to moderate	1—1.5
5	Fresh breeze	Moderate	2—2.5
6	Strong breeze	Rough	3—4
7	Moderate gale	Rough to very rough	4—5.5
8	Fresh gale	very rough to high	5.5—7.5
9	Strong gale	high	7—10
10	Whole gale	Very high	9—12.5
11	Storm	Very high	11.5-16

The relationship between AUV recovery depth and cable length as shown in figure 5:

$$H = L \cos \theta \quad (3)$$

Using a 5 meters long cable to reduce the additional resistance of the recovery cable. When the USV is sailing at the speed of 1m/s on the surface, the force on the V-shaped wing in the water is shown in figure 5. Among them, F_3 is the traction force of the V-shaped wing caused by the cable, and the arm of the center of gravity is L_3 , F_2 is the equivalent resistance when the V-shaped wing moves in the water, and F_1 is the down force generated by the V-shaped wing. The torque of the hydrodynamic force to the center of gravity is M , and the space relationship between the force and moment of the V-shaped wing is equation (4):

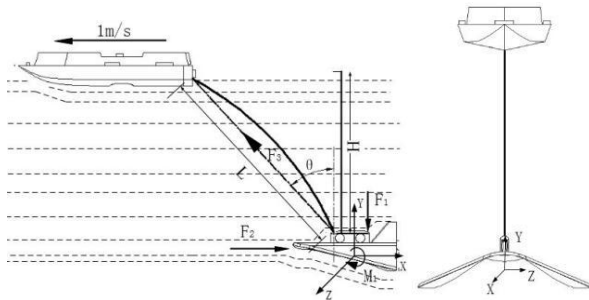


Fig 5. V-wing underwater motion image

$$F_2 = F_3 \sin \theta, \quad F_1 = F_3 \cos \theta, \quad M = F_3 L_3 \quad (4)$$

The cross-section of the middle bulge of the V-shaped wing is shown in figure 6(a), where a_1 is the equivalent radius of the middle raised cross-section, α_1 is the angle of attack at the incoming flow, β_1 is the included angle at the trailing edge, and the two raised cross-sections of the V-shaped wing is shown in figure 6(b), α_2 is the angle of attack at the incoming flow, and β_2 is the angle at the trailing edge.

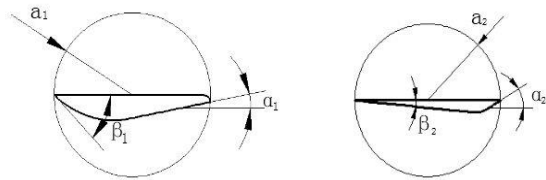


Fig 6(a). the middle bulge Fig 6(b). the raised cross-sections

The working depth of the V-shaped wing is 2 to 5 meters and the velocity of the flow field around it changes slowly. It can be equivalent to quasi-steady flow. The hydrodynamic analysis of V-shaped wings is a cylindrical flow around a quasi-steady flow. The water flow can only smoothly flow through the V-shaped wing trailing edge at a finite speed, according to the Kuta condition assumption^[16], the hydrodynamic F of arbitrary cross-section of the V-shaped wing is equation (5):

$$F = X + iY = 4\pi a |V_\infty|^2 e^{i\left(\alpha + \frac{\pi}{2}\right)} \sin(\alpha + \beta) \quad (5)$$

Where: a is the airfoil equivalent radius. V_∞ is the speed flow from infinity. α is the angle of attack at the incoming flow, and β is the angle at the trailing edge, ρ is the density of water.

The cross-sectional shape parameters of the V-shaped wing have only one variable--the equivalent radius a , the variation range of the middle convex portion a_1 is at 150-205mm, and the variation range of the two-wing convex portion a_2 is 0-140 mm. $\alpha_1 = 31^\circ$, $\beta_1 = 6^\circ$, $\alpha_2 = 20^\circ$, $\beta_2 = 47^\circ$. Because of $\alpha \neq -\beta$, the speed change flow around the airfoil is not equal to zero, and the airfoil down force is not zero.

The force of the V-shaped wing is calculated according to the aerodynamic formula. The down force produced by the V-shaped wing can be expressed as:

$$F = 0.5 C_y \rho V^2 S \quad (6)$$

Where: take C_y is lift coefficient whose value is 0.6, V is dynamic pressure (relative speed) whose value is 1m/s. S is the reference surface area of the V-shaped wing whose value is 0.4 m², ρ is the density of water whose value is 1000kg/m³. Then we can calculate the F :

$$F = 0.5 C_y \rho V^2 S = 0.5 \times 0.60 \times 1 \times 1000 \times 0.4 = 12N$$

The calculation result shows that the down force is 12N when the V-shaped wing moves at the speed of 1m/s. The lift coefficient is the empirical coefficient. To verify the rationality of the empirical coefficient selection, numerical simulation of V - wing is carried out.

III. SIMULATION AND TEST

A. Simulation analysis

CFD fluid analysis software is used to perform hydrodynamic simulations on the V-shaped wing. Pointwise is used to mesh the V-shaped wing, as shown in figure 7. An encryption area is set in the calculation domain to improve calculation accuracy. The mesh size of the encryption area is 2250mm×2000mm×2000mm, while the calculation domain size is 17900mm×10000mm×10000mm, and the number of boundary layers is 10^[17]. In the CFD calculation, the buoyancy of the V-shaped wing in the water is zero, and the solution model is the $k-\omega$ model which is a commonly used turbulence model and can meet the analysis requirements in this study. The speed of the inlet is set to 1.28 m/s and the pressure of the outlet is 0 Pa. figure 7(b) is a partially enlarged view.

The simulation result shows that the V-shaped wing generates down force of 10N and resistance of 12.5N. In order to further study the relationship between the drag speed and the hydrodynamic forces of the V-shaped wing, the V-shaped wing is simulated and analyzed taking the drag speed as input. figure 8 shows the variation of the resistance and the down force generated by the V-shaped wing. Curve A is the down force, and curve B is the resistance. The simulation results show that as the down force and resistance

generated by the V-shaped wing increases with the increase of the drag speed.

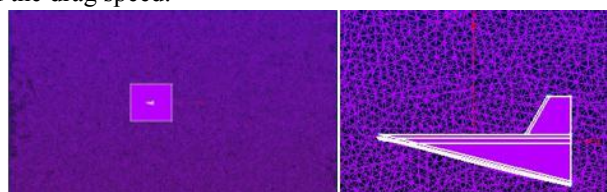


Fig 7(a) Mesh

Fig 7(b) Enlarged view

Figure 7. the V-shaped wing mesh

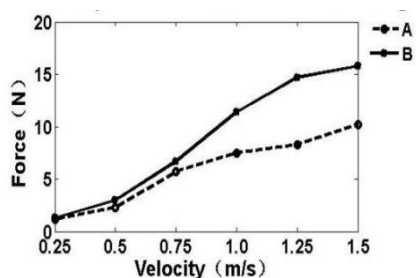


Fig 8. Simulation result

Star ccm+ fluid analysis software is used to perform hydrodynamic simulation analysis on the V-shaped wings to study the down force area generated by V-shaped wing. The software parameter setting is the same as CFX. The motion parameters of the V-shaped wing are unchanged (2 knots, 0 attack angle drag). The simulation results are shown in figure 9. At the bottom of the V-shaped wing, all the three raised parts produce a green low-pressure zone, which is the key for the V-shaped wing to generate the down force. To further verify the performance of the V-shaped wing, the water test is conducted.

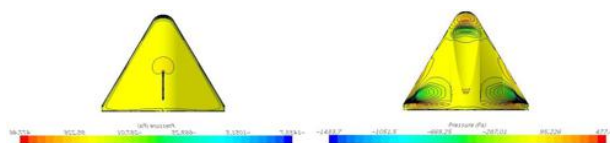


Fig 9. Star ccm+ simulation result

When the portable AUV approach the V-shape wing, it would be disturbed by the wake flow of the v-shaped wing. So we simulation the resistance of the AUV when it approach the V-shaped wing. Using the star ccm+ mesh the 3D model and set the motion speed of AUV in the computational domain to 1m/s, the computational domain inlet velocity to 0.5kn, 1kn, 1.5kn and 2kn respectively, the grid is shown in figure 10



Fig 10. Grid model of AUV and the V-shaped wing

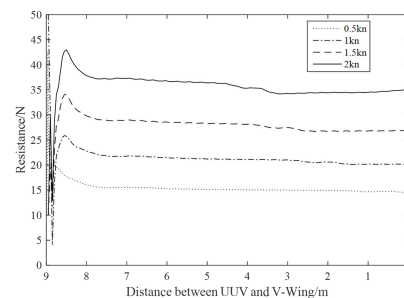


Figure 11. AUV resistance when approaches the V-shaped wing

B. The water test

The V-shaped wing is 3D printed using polylactic acid (PLA) with a density of 1.3 kg/L, as shown in figure 12. In order to make the V-shaped wing in neutral buoyancy condition, the filling rate is set to 70% (density: 0.91 kg/L) at the time of printing. At this filling rate, the V-shaped wings exhibited a slightly positive buoyancy state.



Fig 12. 3D printed V-shaped wing

The water test is performed with the printed V-shaped wing to measure the actual down force generated by the V-shaped wing and its motion stability. A depth transducer measuring the real-time depth and depth stability. The V-shaped wing is connected to the surface USV through five-meter long cable. The depth transducer is connected to the V-shaped wing through a thin cable with diameter of 4 mm and length of 150 mm. A tension sensor is connected between the cable and the USV to measure the pull force generated when the V-shaped wing moves. figure 13 shows the external water test scenario.



Fig 13. Field test scene

The figure 11 shows the simulation results. From the results, we can see that when the AUV approach the V-shape wing, the resistance of the AUV would suddenly increase, so the AUV should enter the docking height ahead of time.

In the water test, part of the test data obtained by the tension sensor and depth transducer is shown in table 4. After two calculations of the trigonometric function shown in figure 14, we can obtain the down force generated when the V-shaped wing is dragged. In figure 15, curve A is the down force without the V-shaped wing and the curve B is the down force when dragging the V-shaped wing. The data curve in Fig 10 shows that: (1) The V-shaped wing can generate down

force when it moves; (2) When the V-shaped wing moves faster, the down force generated by the V-shaped wing increases.

Relationship between depth and speed is shown in figure 16. From the curve of figure 16, the V-shaped wing can maintain at certain depth and keep stability when the drag velocity is stable. The test results are basically consistent with the simulation results, and the error is within the allowable range.

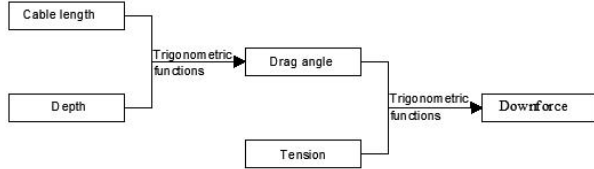


Fig 12. Pressure calculation process diagram

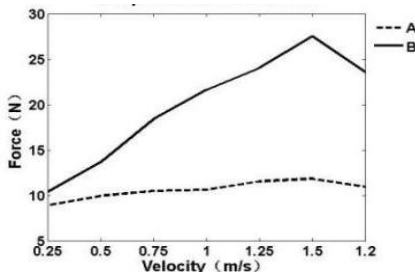


Fig 13. With or without V-wing pressure comparison chart

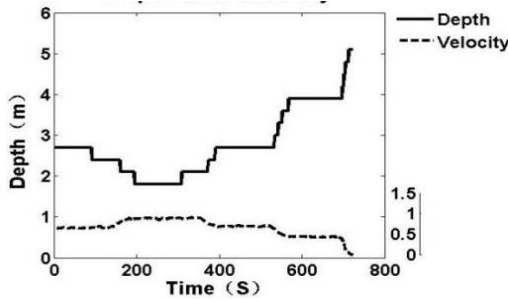


TABLE 4. MEASURED DATA

Drag without V-shaped Wing				Drag at the point 1			
Depth (m)	Tension (N)	Length (m)	Angle (°)	Depth (m)	Tension (N)	Length (m)	Angle (°)
5.6	09.95	5.9	66.24	5.6	11.2	5.9	66.37
5.5	10.9	5.9	63.78	5.3	15.5	5.9	64.94
5.2	12.15	5.9	61.81	4.3	24.6	5.9	49.79
4.6	13.9	5.9	57.23	3.8	32.9	5.9	48.83

Fig 14. V-wing depth and velocity image

IV. CONCLUSION

In this paper, we design a V-shaped type moving base for AUVs recovery. The Bernoulli equation of the ideal fluid is taken as the design concept, and the balance of space force systems is the design principle. The hydrodynamic analysis

software is used to analyze the V-shaped wing and calculation results show that with the increasing of the drag speed, the down force generated by the V-shaped wing getting larger. The accuracy of the simulation results and the stability of the device are verified through the water test. We can draw the following conclusions:

(1) The V-shaped wing uses a triangular structure. After dynamic analysis and calculation, the V-shaped wing has a righting torque during operation, which ensures that the V-shaped wing can run stably when towed. The bottom bulge can provide down force, enabling the recovery cable is always tight, allowing the AUV to capture the recovery cable.

(2) As the towing speed of USV increases, the lift-to-drag ratio of V-shaped wing will decrease gradually. When the USV towing speed is stable, V-shaped wing can be stabilized at a fixed depth, and the moving base is in dynamic stability, ensuring the relative position of the recovery cable fixed and successful capture and recovery.

V. FUTURE WORK

Because the V-shaped wing attitude device is not measured during the field test, it is difficult to obtain its true motion state. In the follow-up, tcm5 and fin rudder will be installed on the V-shaped wing to control its underwater movement posture and adapt to the AUV self-recovery work under higher sea conditions.

REFERENCES

- [1] J.Du. "Design and hydrodynamic analysis of AUV self-recovery device for USV". *Chinese Journal of Engineering Design*. vol.25, no.1, pp.35-42, Feb. 2018.
- [2] Li D J, Chen Y H, Shi J G. "Autonomous underwater vehicle docking system for cabled ocean observatory network". *Ocean Engineering J.* pp:127-134,2015.
- [3] Stokey R, Purcell M, Forrester N. "A docking system for REMUS, an autonomous underwater vehicle". *Oceans. IEEE.C.* vol.2, pp.1132-1136,2002.
- [4] Palomeras N. "Autonomous I-AUV Docking for Fixed-Base Manipulation". *World Congress.C.* pp.12160-12165,2014.
- [5] Piskura J C, Purcell M, Stokey R. "Development of a robust Line Capture, Line Recovery (LCLR) technology for autonomous docking of AUVs". *Oceans. IEEE.C.* pp.1-5,2016.
- [6] B.Allen. "Autonomous Docking Demonstrations with Enhanced REMUS Technology". *OCEANS. IEEE. C.* pp.1-6,2006.
- [7] B.Nye. Circle "UNDERWATER MOBILE DOCKING OF AUTONOMOUS UNDERWATER VEHICLES". *OCEANS IEEE MTS C.* pp.15, Oct 14-19. 2012.
- [8] El.Sarda, MR.Dhanak. "A USV-Based Automated Launch and Recovery System for AUVs". *OCEANIC ENGINEERING.J.* vol.42, no.1, pp.37-55, Jan. 2017.
- [9] Sarda E, Dhanak M. "CONCEPT FOR A USV-BASED AUTONOMOUS LAUNCH AND RECOVERY SYSTEM" *Launch and Recovery. C.* 2015.
- [10] Klinger W B, Bertaska I R, Ellenrieder K D V. "Experimental testing of an adaptive controller for USVs with uncertain displacement and drag". *Oceans. IEEE. C.* pp.1-10, 2015.
- [11] Dan M L, Jacobson J, Hardy M. "Autonomous Inspection Of Undersea Structures" *Sea Technology.J.* vol.55, no.4, pp.39-41, 2014.
- [12] Sharp K, Cronin D, Small D, et al. "A cocoon-based shipboard launch and recovery system for large autonomous underwater vehicles" *Oceans. IEEE.C.* vol.1, pp.550-554, 2002.
- [13] SE.Sarda, M.Dhanak, and K.V.Ellenrieder, "CONCEPT FOR A USV-BASED AUTONOMOUS LAUNCH AND RECOVERY SYSTEM" *Launch And Recovery* 2014, ASNE

- [14] X.X.Du, B.W.Song, MENG Rui and LI Jia-wang ,“Effect of Wave to Low Speed Maneuvers of Torpedo-like Long-distance AUV”*Journal of System Simulation*.J.vol. 20, no. 8,pp.1945-1949,Apr .2008
- [15] DK.Chen ,“Coastal engineering”,Science press,2017,pp.56-59.
- [16] LX.Zhuang,XY Yin, and HY Ma, “hydromechanics”China science and technology university press,2012,pp.188-190.
- [17] ZhQ.Hu, “Numerical Calculation Methods for Hydrodynamics of Unmanned Marine Vehicles and their Application”Ph.D.dissertation, Dept. SIA. China,University of Chinese academy of sciences, Beijing,2013